



YoMaHa'07:

**Velocity data assessed from trajectories of Argo floats
at parking level and at the sea surface**

**Konstantin V. Lebedev,
Hiroshi Yoshinari, Nikolai A. Maximenko, and Peter W. Hacker**

IPRC Technical Note No.4(2)

June 12, 2007

Konstantin V. Lebedev, Hiroshi Yoshinari, Nikolai A. Maximenko, and Peter W. Hacker, 2007: YoMaHa'07: Velocity data assessed from trajectories of Argo floats at parking level and at the sea surface, IPRC Technical Note No. 4(2), June 12, 2007.

Abstract

This variant of technical paper accompanies the release of public dataset YoMaHa'07 (the update of YoMaHa'05) and provides a brief description of its structure and the techniques used for its preparation. The dataset contains estimates of velocities of deep and surface currents obtained using data of the trajectories from Argo floats. It includes data from 4284 floats stored in nine Data Assembly Centers (DAC's) worldwide and about 297,000 values of velocity. This is a 41% increase in the number of floats and 78% increase in the amount of data compared to YoMaHa'05. The data span the period from August 04, 1997 through May 15, 2007. Surface velocities are linearly regressed from float coordinates fixed by the ARGOS satellites. Deep velocities are estimates from floats displacements during each submerged phase of the cycle. Both surface and deep velocities are accompanied by error estimates, which are typically an order of magnitude smaller than velocity values. The paper describes data distribution in space, time and between the DAC's as well as probability distributions of programmed float parameters and statistics of their displacements. Possible application of the dataset is illustrated on the example of the ensemble-mean velocity field.



Table of content

1.	Introduction.....	1
1.1	What is Argo?.....	1
1.2	Argo data flow.....	1
1.3	Float design and data format.....	1
2.	YoMaHa'07 dataset.....	2
2.1	Argo array description and problems with data at DAC's.....	2
2.2	Characteristics of YoMaHa'07 dataset.....	3
2.3	Applications.....	8
2.4	Format of YoMaHa'07 dataset.....	10
3.	Acknowledgments.....	13
4.	Appendices.....	13
4.1	Appendix A. Error assessment of deep velocity due to vertical shear of horizontal flow.....	13
4.2	Appendix B. Assessment of surface velocity and its error.....	14
5.	References.....	15
6.	Contacts.....	16
7.	Copyright.....	16

1. Introduction

1.1. What is Argo?

Argo is an international program providing a near real-time assessment of the state of global ocean from an array of autonomous profiling floats. Program began in 2000 and the number of active floats grows

fast having reached 2852 floats by the time of this writing. Their positions are shown in Figure 1. When the array will reach the target number of 3000, it will be providing data on a roughly 3° global grid.

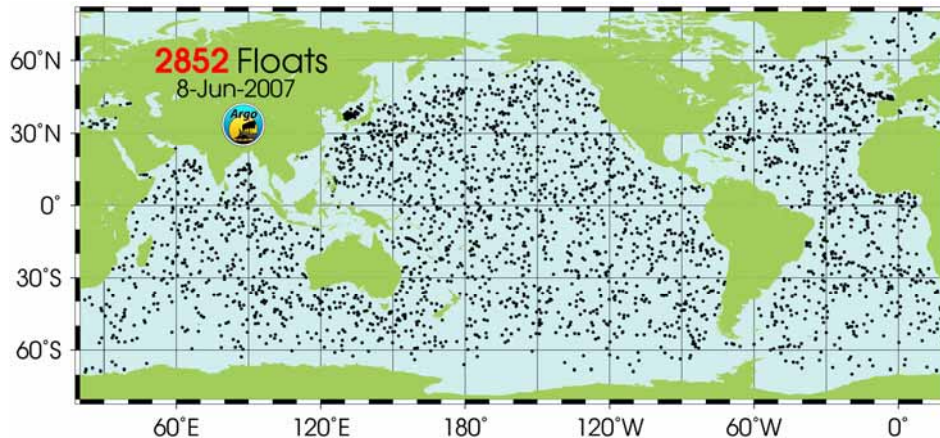


Figure 1. Distribution of active Argo floats (the floats that have delivered data within the last 30 days) on June 8, 2007 (image downloaded from http://www.argo.ucsd.edu/FrAbout_Argo.html)

1.2. Argo data flow

The array consists of coordinated regional deployments and is made up of 25 different countries' contributions. The U.S. contribution is about 50% of the global array. Raw data are publicly available in near real-time via the Global Telecommunications System. 24 hours later, real-time quality controlled trajectory data are stored at nine national/regional Data Assembly Centers

(DAC's), which also provide ultimately corrected profile data with a few months delay. The data also include pre-Argo floats of similar design. Two GDAC's (global DAC's), USGODAE and IFREMER, manage global Argo dataset compiled of folders-images of the nine DAC's. In the U.S.A., the ftp gate to the data is <http://www.usgodae.org/ftp/outgoing/argo/>.

1.3. Float design and data format

There are three main types of Argo floats (APEX, SOLO and PROVOR) and at least six other types that differ in nuances. Common among all the floats is that they are able to change their buoyancy by pumping water in and out of an external bladder and are designed to spend most of their lifetime on some pre-selected isobaric surface (so-called, parking pressure). During the ascent, the float measures and stores a CTD profile that is transmitted to ARGOS satellite when the float reaches the sea surface. Same satellite detects coordinates of the float as long as the latter drifts at the sea surface. The floats thus work in cycles. Schematic of a typical cycle is shown in

Figure 2. The n-th cycle starts (a time T_{dive}^n) when a float begins to descend from the sea surface to the parking level (which it reaches by time T_{beg}^n). As a rule just before the beginning of the ascent, a float dives (at time T_{end}^n) to a slightly larger depth. As it surfaces at T_{surf}^n , it starts transmitting data. It stays at the sea surface long enough to insure that ARGOS satellites will receive the information. Transmissions stop with the beginning of the next, n+1-th cycle at T_{dive}^{n+1} . T_{first}^n and T_{last}^n indicate in Figure 2 first and last transmissions, respectively, received (fixed) by satellite during the n-th cycle of the float. As a rule more than two transmissions are received.

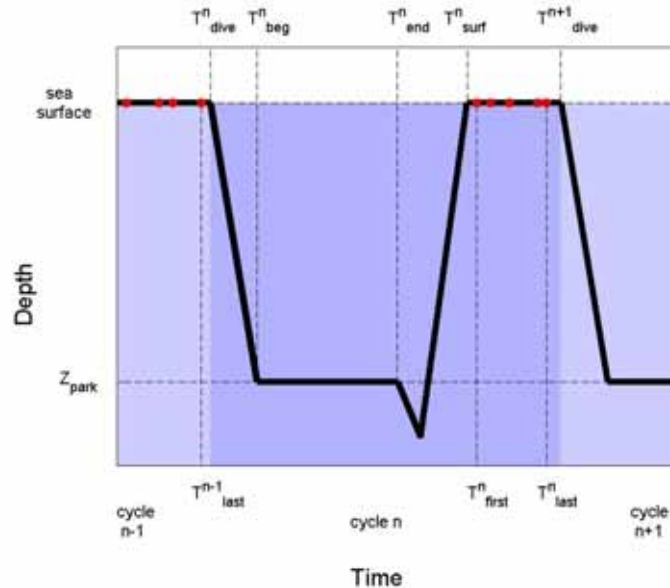


Figure 2. Time-depth schematic of a float cycle. Red dots mark satellite fixes of the float at the sea surface.

Data from the float are stored in files of four different types: meta, profile, trajectory and technical files. “Meta” file contains pre-programmed information on the float cycles. Data of individual CTD-profiles are stored in the “profile” files (one per a cycle) and can be used just like ship-borne CTD data. At present, profile data is the most heavily used output of the Argo program. Trajectory (“traj”) file contains information on three-dimensional movement of the float. It basically consists of a set of coordinates of the float during its transmissions from the sea surface and, in some instances, recorded pressure during the

“parked” phase of the cycle. By itself, description of the float trajectory in the “traj”-file is largely incomplete. Typical duration of the cycle is 10 days and, to ensure successful reception of data, a typical stay at the sea surface is between 12 and 24 hours. In most cases, a float is programmed to repeat the same cycle. However, in some instances parking pressure was programmed to vary cycle to cycle. Cycle duration and parking pressure also change as the float deteriorates and as it moves from one water mass to the other [e.g., Park et al., 2005b].

This work is an attempt to extract information on surface and deep velocities using simple assumptions in application to Lagrangian part of the Argo floats. To the best of our knowledge this is the first such database utilizing data stored in all Argo DAC’s and covering the whole World Ocean.

2. YoMaHa'07 dataset

2.1. Argo array description and problems with data at DAC’s

We started at <http://www.usgodae.org/ftp/outgoing/argo/> and have downloaded all data available at all nine DAC’s on May 16, 2007. It included data of 4284 floats ranging from August 04, 1997 through May 15, 2007. Data from individual floats received from different DAC’s

were converted into same format and merged. This procedure was complicated by differences between processing techniques and actual formats of “trajectory” data in different DAC’s. In addition, a number of apparent errors have been found in the quality-controlled data. These include:

- Time inversion/duplication

In some trajectory files the timeline is not monotonic. This is due to the errors in the time values, not a matter of the order of lines in the file. At time of YoMaHa'05, this problem was most serious in the data of INCOIS, but similar problems (mostly duplicates) were also detected in data of all DAC's and in 14% of all cycles. In this database we flag

cycles with time problem and will address the problem more adequately in future. In addition, problem appeared in the recent version of INCOIS files containing wrong julian time. When possible, we used old, better, version of the problematic files and notified the DAC about the error.

- Coordinate spikes

In a number of cases large jumps in float coordinates were detected. In simple cases, corrections have been made by comparing with

the "profile" files. BODC DAC has been notified about the problem in their data and corrected files were submitted to BODC.

2.2. Characteristics of Yomaha'07 dataset

Dataset Yomaha'07 contains data of 4284 floats stored in the DAC's. Total number of cycles in YoMaHa'07 is 296974, 290247 of which provided estimates of velocity at a float's parking depth, 294201 provided estimates of surface current and 287474 provided both deep and surface velocities during the same cycle.

As shown in Figure 3, the DAC at AOML contains 52% of the Argo float data and AOML, CORIOLIS and JMA together provide about 84%. However, Figure 4 illustrates that smaller datasets of the six other DAC's are important in a number of regions.

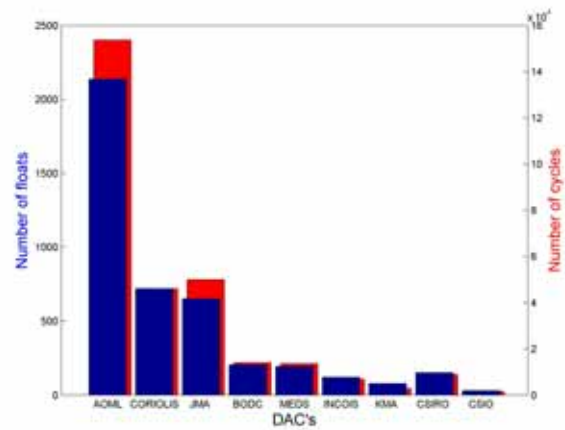


Figure 3. Number of floats and their cycles stored at individual DAC's and included into YoMaHa'07 dataset.

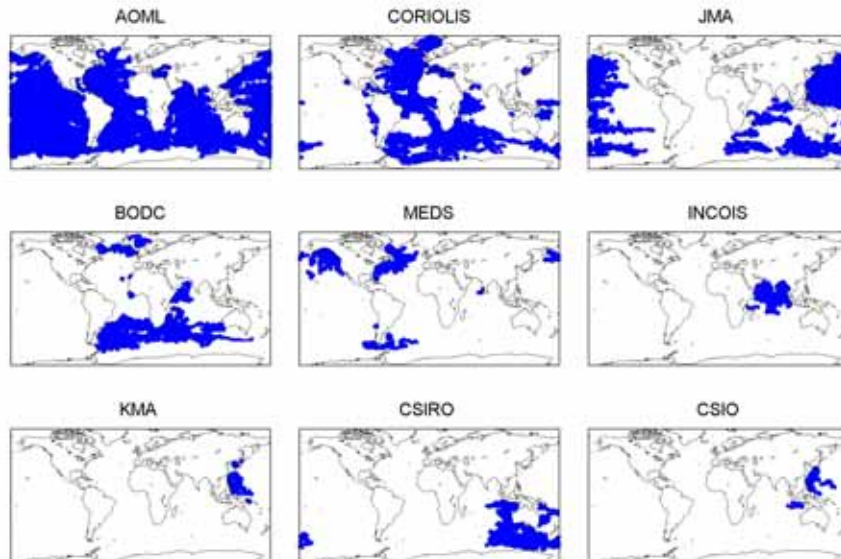


Figure 4. Data distribution between the Argo DAC's. Shown are locations of velocity estimates at parking depth gathered in YoMaHa'07.

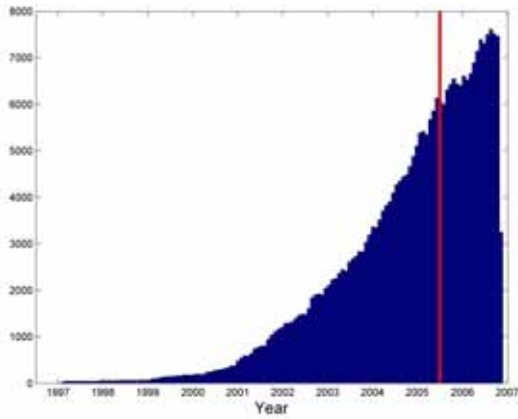


Figure 5. Monthly number of the float cycles stored in YoMaHa'07. Red line marks the end of the period covered by YoMaHa'05.

Figure 5 shows the growing number of cycles available for velocity estimates. Annual coverage of the World Ocean with the data is presented in Figure 6.

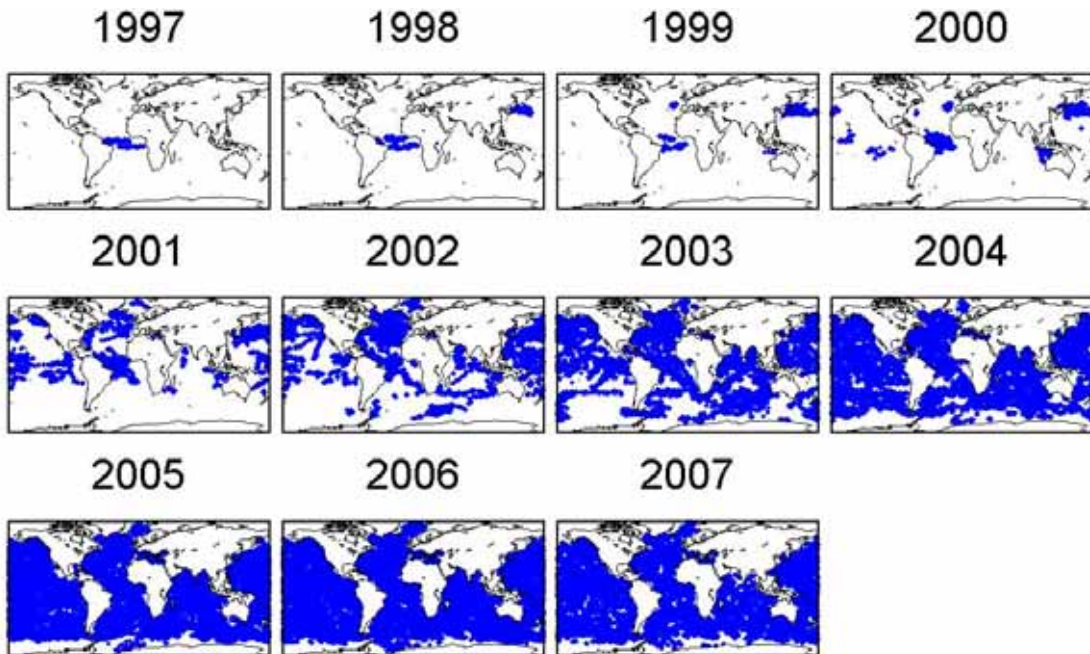


Figure 6. Annual distribution of Argo velocity estimates in YoMaHa'07.

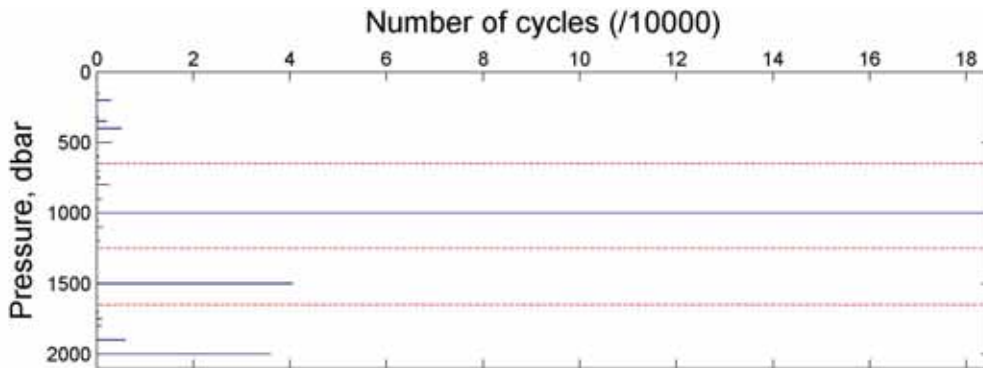


Figure 7. Number of cycles in 10-dbar intervals of the float parking pressure. Red dashed lines separate four layers selected for Figure 8.

As seen in Figure 7, the majority of the data in YoMaHa'07 came from the floats programmed for the parking pressure 1000 dbar (63% of total data volume), 2000 dbar (12%) and 1500 dbar (14%). Horizontal distribution of Argo floats in different layers is shown in Figure 8.

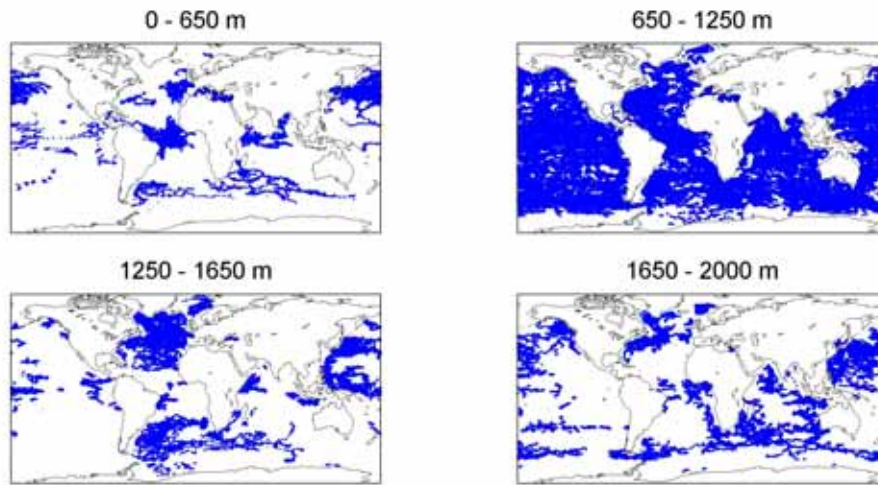


Figure 8. Distribution of Yomaha'07 deep velocity data in four layers shown in Fig.7.

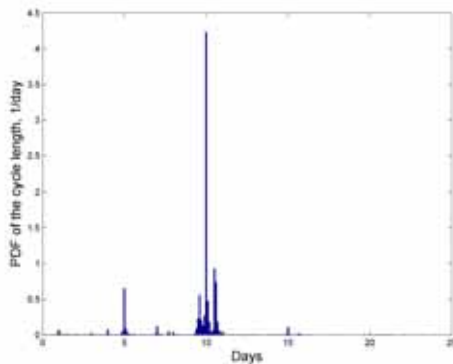


Figure 9a. Probability density function (PDF) of float cycle lengths stored in YoMaHa'07. Average value is 9.5 days, 85% of values lie between 8.9 and 11.5 days.

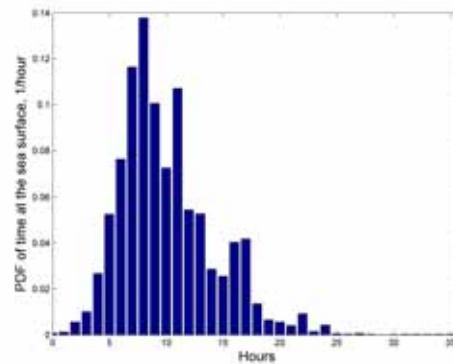


Figure 9b. PDF of duration of float stay at the sea surface. Average value is 10.1 hours.

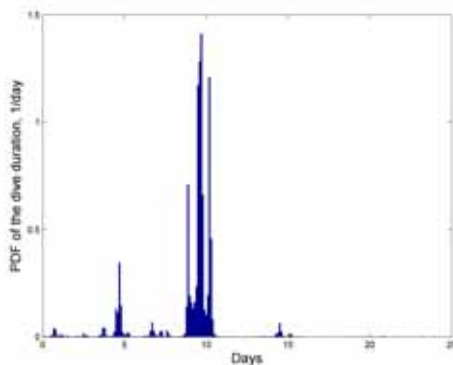


Figure 9c. PDF of float stay under water. Average value is 9.1 days.

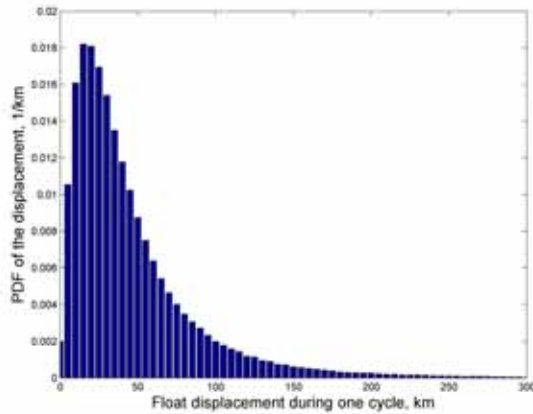


Figure 10a. PDF of displacement during one cycle. Mean value is 45.4 km.

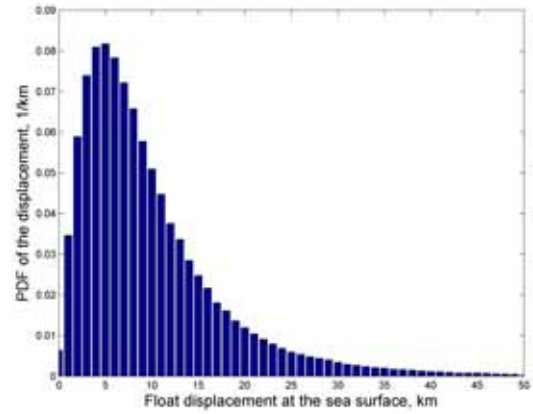


Figure 10b. PDF of displacement at the sea surface. Mean is 9.7 km.

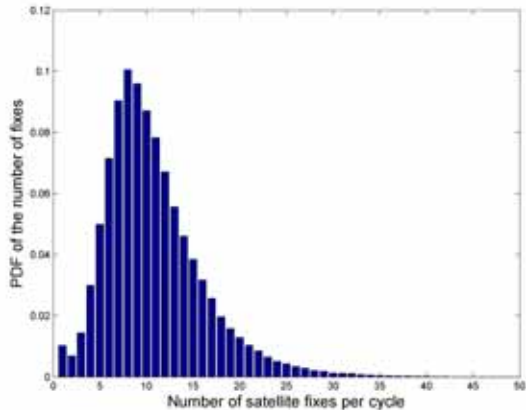


Figure 10c. PDF of the number of transmissions received by ARGOS satellite from the float during its stay at the surface during one cycle. Mean is 10.8 fixes.

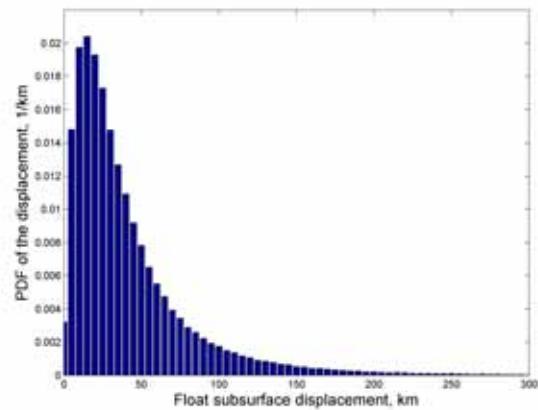


Figure 10d. PDF of the float displacement while submerged. Mean is 41.0 km.

As follows from Figures 9 and 10, a typical float included into the YaMaHa'07 dataset most probably is programmed for a 10-day cycle with 8-hour duration of the surface phase. During one cycle the float moves over the distance about 15 km, most of which it makes underwater. Displacements at the sea surface, during which the float will most likely send eight successful messages to the satellite, is approximately 4 km. As all variables, whose probability distributions are shown in Figures 9 and 10, are essentially positive, their statistics are naturally skewed toward larger values, so that mean values exceed corresponding most-probable ones by a factor of 1.2-2.5.

Of particular importance are statistics of velocities that are the essence of this dataset. Probability density function of velocity estimates at parking level shown in Figure 11a has its maximum around 2 cm/s. The weakness of deep currents makes their velocity estimates sensitive to many known and unknown errors. Unlike trajectories of SOFAR or RAFOS

floats, trajectories of Argo floats are essentially three-dimensional. During ascending/descending phases of the cycle floats are subject to effect of not only vertically sheared geostrophic currents, but also Ekman currents, inertial oscillations and other processes specific to the upper ocean (*e.g.*, Park et al. [2004, 2005a]). Given the complexity of the

situation, certain optimism comes from Figure 11b, which shows that simple estimates of velocity error have most probable value of 0.25 cm/s and mean 0.53 cm/s. An order of magnitude difference between the velocity and its error allows sensible quantitative estimates even when a preliminary, simple technique

is employed. According to Figure 11c, most probable relative error of the velocity at parking pressure (i.e., error-to-velocity ratio) is 0.03 (3%), 54% of deep velocity data have relative error less than 10% and 97.6% of the data have velocity error smaller than velocity value.

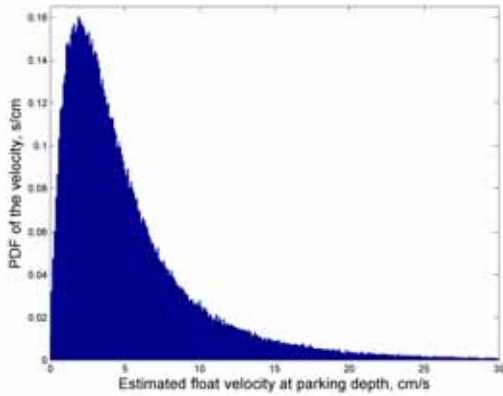


Figure 11a. PDF of deep velocity. Mean is 5.5 cm/s.

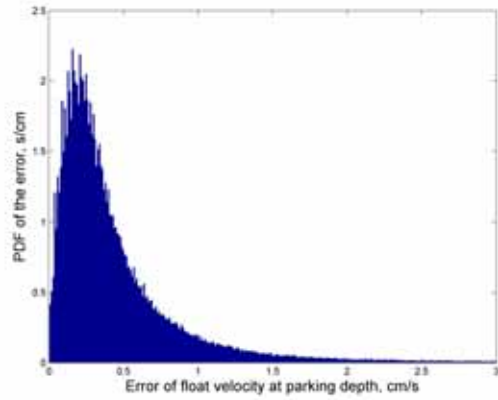


Figure 11b. PDF of error of estimate of deep velocity due to baroclinicity (as described in Appendix B). Mean is 0.53 cm/s.

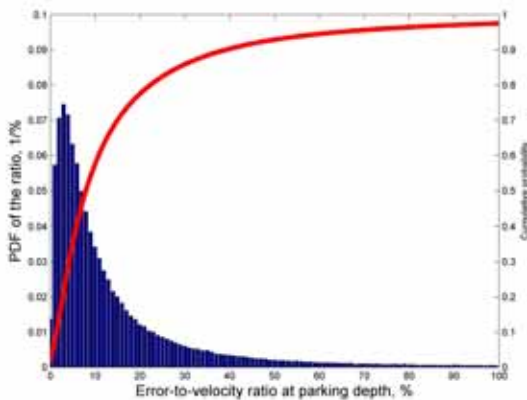


Figure 11c. PDF of relative velocity error (in %) at the parking depth (blue bars and left y-axis) and cumulative probability (in %, red line and right y-axis).

As shown in Figure 12 most probable surface velocity is about 20 cm/s and its mean value is 28.2 cm/s. Probability of surface velocity error peaks at 1.9 cm/s and the mean error value is 2.9 cm/s. Similarly to deep velocities, surface velocities exceed their errors by an order of magnitude. Higher-order

techniques [Park et al., 2005a] may further improve the confidence of the surface velocity data. According to Figure 12c, most probable relative error of the velocity at the sea surface is 0.06 (6%), 45% of surface velocity data have relative error less than 10% and 98.8% of the data have velocity error smaller than velocity value.

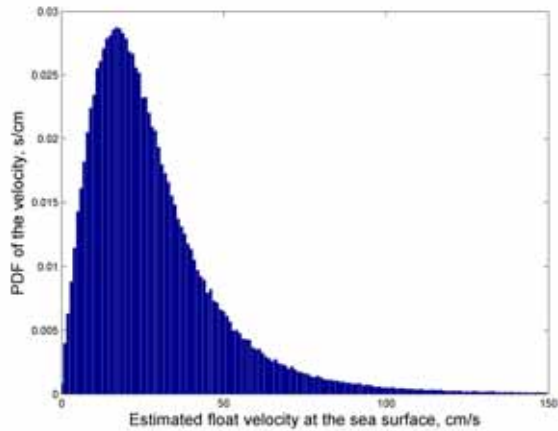


Figure 12a. PDF of surface velocity. Mean is 28.2 cm/s.

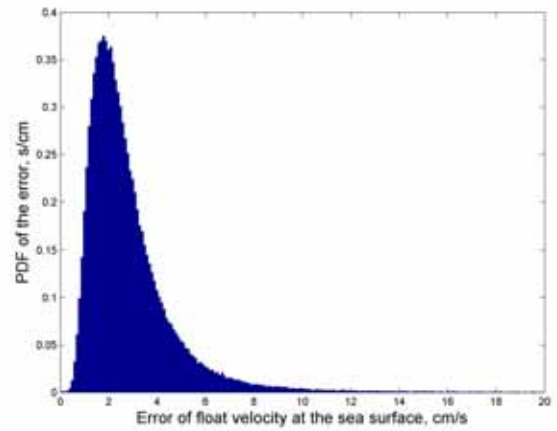


Figure 12b. PDF of error of estimate of surface velocity. Mean is 2.9 cm/s.

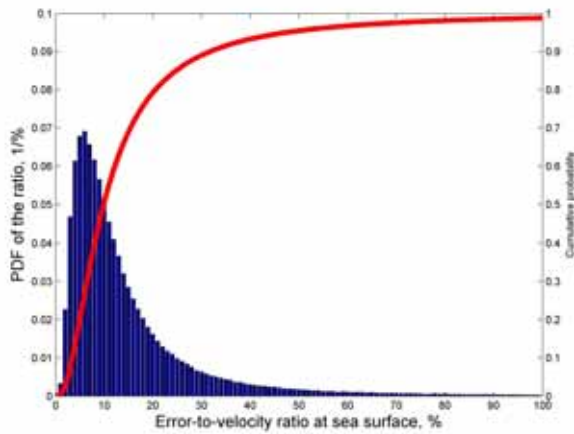


Figure 12c. PDF of relative velocity error (in %) at the sea surface (blue bars and left y-axis) and cumulative probability (in %, red line and right y-axis).

2.3. Applications

To illustrate possible application of data in YoMaHa, we calculated mean velocity based on the previous version YoMaHa'05, both in the deep and at the sea surface, by averaging data in bins of size $3^\circ \times 3^\circ$. For deep velocities we used all data with parking pressure larger than 750 dbar and deep velocity error smaller than 2 cm/s. For surface velocities we used all data with the surface velocity error less than 15 cm/s. Figure 13 shows surface circulation pattern similar to the one observed with surface drifters [Maximenko

and Niiler, 2005]. Deep currents in Figure 13b are extraordinarily strong in the Antarctic Circumpolar Current and contain a number of peculiar structures emerging from the generally noisy patches. The latter structures are beyond the scope of this dataset documentation and are a subject of our future study. At present it is not clear whether the noise is due to data distribution, related to mesoscale eddies or a consequence of errors in our data and methods.

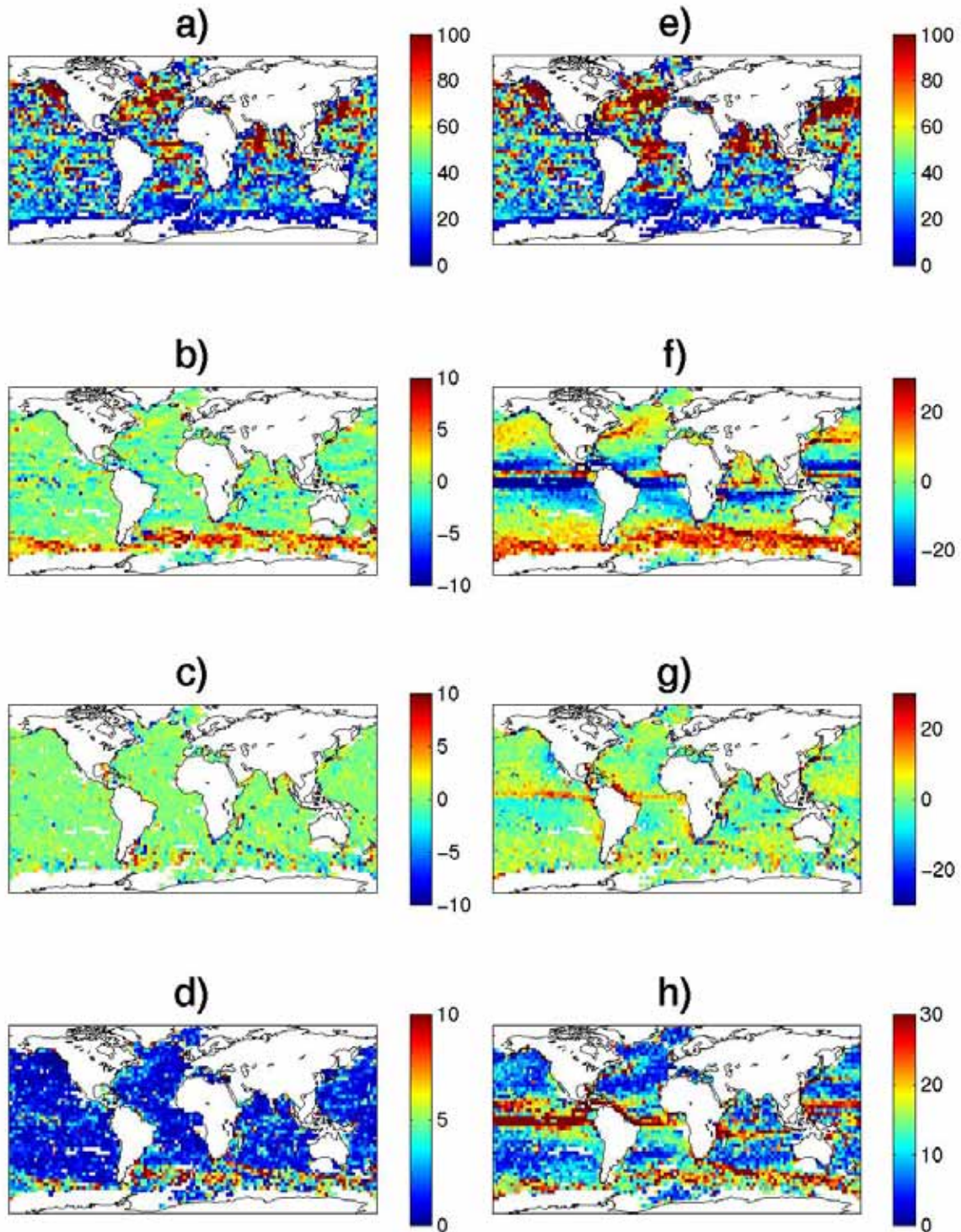


Figure 13. Argo velocity statistics in $3^\circ \times 3^\circ$ bins estimated from YoMaHa'05. Left column is for parking level, right is for sea surface. Rows are number of cycles falling into the bin (top, *a,e*), mean zonal (*b,f*) and meridional (*c,g*) velocity components, and magnitude of mean velocity (bottom, *d,h*). Units of velocities are cm/s. Deep velocities with the error larger than 2 cm/s and surface velocities with the error larger than 15 cm/s are disregarded.

2.4. Format of YoMaHa'07 dataset

YoMaHa'07 dataset is a set of velocity estimates at random times and locations. The technique that we employed was targeted at flow velocity assessment at the float parking pressure and, independently, at the sea surface. However, to make the comparison between surface and deep currents simpler, we sorted all the data according to the float number and the cycle number.

The dataset consists of nine files:

- yomaha070612.dat
- yomaha2wmo_070612.dat
- DACs_060227.txt
- float_types_070612.txt
- MeanVpark3x3_060227.dat
- MeanVsurf3x3_060227.dat
- Copyright_070612.txt
- YoMaHa070612.pdf
- Sample_060227.f

2.4.1. File **yomaha070612.dat** is an ASCII file containing 28 following columns (same as YoMaHa'05).

Columns 1-8 contain three-dimensional coordinates, time, components and errors of the deep float velocity.

1-2. Coordinates (longitude X_{deep}^n and latitude Y_{deep}^n) of location where deep velocity is estimated. These coordinates are averages between last fixed float position (X_{last}^{n-1} , Y_{last}^{n-1}) at the sea surface during previous cycle (stored in columns 16-17) and first fix (X_{first}^n , Y_{first}^n) in the current cycle (stored in columns 19-20).

I.e., $[X, Y]_{\text{deep}}^n = ([X, Y]_{\text{last}}^{n-1} + [X, Y]_{\text{first}}^n) / 2$.

3. “Parking” pressure Z_{park} (dbars) for this cycle. This value is a pre-programmed value stored in the “meta”-file.

4. Julian time T_{deep}^n (days) relative to 2000-01-01 00:00 UTC. (Adding 18262 will convert it into more traditional Julian time relative to 1950-01-01 00:00

UTC.) This value is an average between the Julian time of the last fix during the previous cycle (T_{last}^{n-1} stored in column 18) and the first fix in the current cycle (T_{first}^n stored in column 21). I.e., $T_{\text{deep}}^n = (T_{\text{last}}^{n-1} + T_{\text{first}}^n) / 2$.

5-6. Estimate of eastward and northward components of the deep velocity (U_{deep}^n , V_{deep}^n) (cm/s) at Z_{park} calculated from the float displacement from $[X, Y]_{\text{last}}^{n-1}$ to $[X, Y]_{\text{first}}^n$ for time $T_{\text{first}}^n - T_{\text{last}}^{n-1}$.

7-8. Estimates of the errors of components of deep velocity ($\epsilon_{U_{\text{deep}}}^n$, $\epsilon_{V_{\text{deep}}}^n$) (cm/s) due to a vertical shear of horizontal flow obtained as described in Appendix A.

Columns 9-15 contain horizontal coordinates, time, components and errors of the float velocity at the sea surface. Velocity is estimated using linear regression of all surface fixes for the cycle. Details are given in Appendix B.

9-10. Coordinates (longitude X_{surf}^n and latitude Y_{surf}^n) of location where surface velocity is estimated.

11. Julian time T_{surf}^n (days) relative to 2000-01-01 00:00 UTC when surface velocity is estimated.

12-13. Estimate of eastward and northward components of velocity (U_{surf}^n , V_{surf}^n) (cm/s) at the sea surface.

14-15. Estimates of the errors of components of surface velocity ($\epsilon_{U_{\text{surf}}}^n$, $\epsilon_{V_{\text{surf}}}^n$) (cm/s) obtained as described in Appendix B.

Auxiliary **float and cycle data** are in **columns 16-27**.

16-18. Coordinates (X_{last}^{n-1} , Y_{last}^{n-1}) and Julian time T_{last}^{n-1} (relative to 2000-01-01 00:00 UTC) of the last fix at the sea surface during the previous cycle.

19-21. Coordinates (X_{first}^n , Y_{first}^n) and Julian time T_{first}^n (relative to 2000-01-01 00:00 UTC) of the first fix at the sea surface during the current cycle.

22-24. Coordinates (X_{last}^n, Y_{last}^n) and Julian time T_{last}^n (relative to 2000-01-01 00:00 UTC) of the last fix at the sea surface during the current cycle.

25. Number of surface fixes N_{fix}^n during the current cycle.

26. Float ID. To unify data of all DAC's we re-counted all the floats. Correspondence between our float ID's and WMO float ID's used by the DAC's is described in our file

yomaha2wmo.dat

27. Cycle number. We adopted cycle numbers recorded in data of the DAC's.

28. Time inversion/duplication flag F_i . $F_i = 1$ if at least one duplicate or inversion of time is found in the sequence containing last fix from the previous cycle and all fixes from the current cycle. Otherwise, $F_i = 0$.

Missing cycles

Our float ID number increases monotonically throughout yomaha070612.dat from 1 to 4284, and cycle number increases monotonically within data of

each float. However, not all cycles are recorded, only the cycles, data from which allowed an estimate of at least one (deep or surface) velocity.

Missing values

The following values are used to mask missing values:

- **longitudes**, $X_{deep}^n, X_{surf}^n, X_{last}^{n-1}, X_{first}^n$, and X_{last}^n (columns 1, 9, 16, 19 and 22): -999.9999

- **latitudes**, $Y_{deep}^n, Y_{surf}^n, Y_{last}^{n-1}, Y_{first}^n$, and Y_{last}^n (columns 2, 10, 17, 20 and 23): -99.9999

- **Julian times**, $T_{deep}^n, T_{surf}^n, T_{last}^{n-1}, T_{first}^n$, and T_{last}^n (columns 4, 11, 18, 21 and 24): -999.999

- **parking pressure**, Z_{park} (column 3): -999.9

- **velocity components**, $U_{deep}^n, V_{deep}^n, U_{surf}^n$, and V_{surf}^n (columns 5, 6, 12, and 13): -999.99

- **velocity errors**, $\varepsilon_{U_{deep}}^n, \varepsilon_{V_{deep}}^n, \varepsilon_{U_{surf}}^n$, and $\varepsilon_{V_{surf}}^n$ (columns 7, 8, 14, and 15): -999.99

2.4.2. File **yomaha2wmo_070612.dat** catalogs the float information included into YoMaHa'07 dataset.

This ASCII file contains four columns:

1. Serial YoMaHa'07 number of the float (varies from 1 through 4284).
2. WMO float ID.

3. DAC where float data are stored (from 1 through 9).
4. Float type (from 0 through 9).

2.4.3. File **DACs_060227.txt** describes the notations of the DAC's names, which are as follows:

1. AOML (USA)
2. CORIOLIS (France)
3. JMA (Japan)
4. BODC (UK)
5. MEDS (Canada)

6. INCOIS (India)
7. KMA (Korea)
8. CSIRO (Australia)
9. CSIO (China)

2.4.4. File **float_types_070612.txt** describes the notations of the float types, which are as follows:

- | | |
|-----------|--------------|
| 1. APEX | 6. PALACE |
| 2. SOLO | 7. NINJA |
| 3. PROVOR | 8. NEMO |
| 4. R1 | 9. ALACE |
| 5. MARTEC | 0. METOCEAN* |

* Float 2524 (WMO ID 5900474), whose data are stored in CORIOLIS, has no float type specified in the meta-file. We guessed its type to be METOCEAN based on types of other CORIOLIS floats with close ID numbers.

2.4.5. File **MeanVpark3x3_060227.dat** contains mean velocity values at the parking pressure

larger than 750 dbar averaged throughout the data of file yomaha05.dat within 3°x3° bins. Excluded are only data with error larger than 2 cm/s. File is an ASCII file containing the following five columns:	1. longitude and
	2. latitude of the center of the bin
	3. zonal and
	4. meridional components of the mean velocity
	5. number of data in the bin used for the average.

Left column of Figure 13 illustrates the data of MeanVpark3x3.dat.

2.4.6. File **MeanVsurf3x3_060227.dat** contains mean velocity values at the sea surface

averaged throughout the data of file yomaha05.dat within 3°x3° bins. Excluded are only data with error larger than 15 cm/s. File is an ASCII file containing the following five columns:	1. longitude and
	2. latitude of the center of the bin
	3. zonal and
	4. meridional components of the mean velocity
	5. number of data in the bin used for the average.

Right column of Figure 13 illustrates the data of MeanVsurf3x3.dat.

2.4.7. File **Copyright_070612.txt** describes conditions of use of the dataset YoMaHa'07.

This file must always be in the same directory as file **yomaha070612.dat**.

2.4.8. File **YoMaHa070612.pdf** is a pdf copy of this June 12, 2007 version of the technical note.

2.4.9. File **Sample_060227.f** is a Fortran script illustrating how to access the data stored in YoMaHa'07 files.

2.4.10. File **Update_log.txt** is a new file added to the dataset to document changes in YoMaHa and release of auxiliary files.

3. Acknowledgments

This work was supported by the NOAA, NASA and Japan Agency for Marine-Earth Science and Technology (JAMSTEC) through individual and institutional grants at the International Pacific Research Center (IPRC) within the School of Ocean and Earth Science and Technology (SOEST) at the University of Hawaii.

These data were collected and made freely available by the International Argo Project and the national programs that contribute to it. (<http://www.argo.ucsd.edu>, <http://argo.jcommops.org>). Argo is a pilot program of the Global Ocean Observing System.

The authors thank Sharon DeCarlo (APDRC/IPRC) for her valuable technical help.

The picture on the cover page was compiled using images downloaded from scuba.dvdesign.com and the Argo website.

4. Appendices

4.1. Appendix A. Error assessment of deep velocity due to vertical shear of horizontal flow

We estimate components of deep ($U_{\text{deep}}^n, V_{\text{deep}}^n$) vector at every cycle of the float using its coordinates before it dives and after it re-arrives at the sea surface as

$$(U_{\text{deep}}^n, V_{\text{deep}}^n) = ([X, Y]^n_{\text{first}} - [X, Y]^{n-1}_{\text{last}}) / (T_{\text{first}}^n - T_{\text{last}}^{n-1}) \quad (\text{A.1})$$

This does not account for the fact that velocity varies with depth. Simple estimate of the error of (A.1) due to the vertical shear of horizontal flow can be obtained as follows.

Let's adopt the following assumptions:

- vertical shear of the horizontal velocity is constant in vertical for a given cycle;
- rate V_0 of ascent and descent of the float on corresponding phases of the cycle is constant and is approximately equal to 10 cm/s [Webb, personal communication, 2004];
- differences between last fix and diving times as well as between surface arrival and first fix times are negligible (i.e., communication of the float with satellite is continuous while the former is at the sea surface).

Then deviation of the velocity estimate (A.1) from the true deep velocity ($u_{\text{deep}}^n, v_{\text{deep}}^n$) can be shown to be equal to

$$(U_{\text{deep}}^n, V_{\text{deep}}^n) - (u_{\text{deep}}^n, v_{\text{deep}}^n) = ((U_{\text{surf}}^n, V_{\text{surf}}^n) - (u_{\text{deep}}^n, v_{\text{deep}}^n)) / (T_{\text{first}}^n - T_{\text{last}}^{n-1}) \cdot Z_{\text{park}} / V_0 = \quad (\text{A.2})$$

$$= ((U_{\text{surf}}^n, V_{\text{surf}}^n) - (U_{\text{deep}}^n, V_{\text{deep}}^n)) \cdot \alpha / (1 - \alpha), \quad (\text{A.3})$$

where $(U_{\text{surf}}^n, V_{\text{surf}}^n)$ is velocity at the sea surface, Z_{park} is parking depth and $\alpha = Z_{\text{park}} / V_0 / (T_{\text{first}}^n - T_{\text{last}}^{n-1})$ is a ratio of ascend or descend time to the total time float stays underwater. We define the errors of deep velocity as

$$(\varepsilon_U^n, \varepsilon_V^n) = |(U_{\text{deep}}^n, V_{\text{deep}}^n) - (u_{\text{deep}}^n, v_{\text{deep}}^n)| \quad (\text{A.4})$$

and calculate it using (A.3). Remarkably, the error is proportional to the velocity shear and is defined by duration of the float's vertical excursions. We do not use (A.3) to correct the error because our model is too simplistic. It neither accounts for the real baroclinic structure of the ocean nor discriminates between the Ekman currents, inertial oscillations and geostrophic circulation. In addition, some floats are programmed

to dive to the level deeper than the parking depth before starting their ascent. This may disturb our error estimate, but is not critical as vertical shear of horizontal velocity is largest in the upper ocean.

4.2. Appendix B. Assessment of float surface velocity and its error

We adopt a linear regression least squares method to calculate the surface float velocity V_{surf} and its standard error. y here is a coordinate, t is time and data consist of N pairs of y - t values. Optimal velocity is then the slope of the line minimizing the distance to the data [Weinstein, 1999]

$$V_{\text{surf}} = a = \frac{\sum yt - N\bar{y}\bar{t}}{\sum t^2 - N\bar{t}^2} \quad (\text{B.1})$$

where ' \bar{t} ' and ' \bar{y} ' denote the mean of t and y , respectively.

Standard error $\varepsilon_{V_{\text{surf}}}$ of V_{surf} is

$$\varepsilon_{V_{\text{surf}}} = \sqrt{\frac{SSyy - a \cdot SSy}{N - 2}} \sqrt{\frac{1}{SStt}} \quad (\text{B.2})$$

where

$$SStt \equiv \sum t^2 - N\bar{t}^2, \quad SSyy \equiv \sum y^2 - N\bar{y}^2, \quad SSy \equiv \sum ty - N\bar{t}\bar{y} \quad (\text{B.3})$$

Zonal (meridional) component of surface float velocity and its error were calculated by substituting properly scaled longitude (latitude) data to y in formula (B.1-3). Standard error here includes velocity variations due to inertial oscillations. The latter have been found by Park et al. [2004] to be significantly strong in the Japan/East Sea. However, our Figures 12 *a-c* illustrate that effect of inertial motions on global velocity dataset is relatively small. Unaccounted in this approach is a slip of the float relative to surrounding water under joint force of wind and waves. Similar effect directly measured with near-surface drifters [Niiler et al., 1995] leads to sensible (a few cm/s) values of the slip under moderate (some m/s) winds and can be even stronger for the Argo floats not having (unlike the drifters) the large drogue at 15m depth.

4. References

Maximenko, N.A., and P.P. Niiler, 2005: Hybrid decade-mean global sea level with mesoscale resolution. In N. Saxena (Ed.) *Recent Advances in Marine Science and Technology, 2004*, pp. 55-59. Honolulu: PACON International.

Niiler, P. P., A. S. Sybrandy, K. Bi, P. M. Poulain, and D. Bitterman, 1995: Measurements of water-following characteristics of Tristar and Holey-sock drifters. *Deep-Sea Res.*, **42**, 1951-1964.

Park, J. J., K. Kim, and W. R. Crawford, 2004: Inertial currents estimated from surface trajectories of ARGO floats. *Geophys. Res. Lett.*, **31**, L13307, doi: 10.1029/2004GL020191.

Park, J. J., K. Kim, and B. A. King, 2005a: Global statistics of inertial motions. *Geophys. Res. Lett.*, **32**, L14612, doi: 10.1029/2005GL023258.

Park, J. J., K. Kim, B. A. King, and S. C. Riser, 2005b: An advanced method to estimate deep currents from profiling floats. *J. Atmos. Oceanic Technol.*, **22**, 1294-1304.

Weistein, E.W., 1999: The CRC concise encyclopedia of mathematics, Chapman & Hall/CRC, p.1047.

5. Contacts

Comments, questions regarding the YoMaHa'07 dataset and requests for the data can be directed to any of the authors.

Konstantin Lebedev, Nikolai Maximenko, and Peter Hacker are affiliated at IPRC/SOEST, University of Hawaii, 1680 East West Road, POST Bldg. #401, Honolulu, HI 96822-2327, USA

Hiroshi Yoshinari works at Physical Oceanography Section, Marine Productivity Division, National Research Institute of Fisheries Science, Fisheries Research Agency, 2-12-4 Fukuura, Kanazawa-ku, Yokohama 236-8648, Japan.

The authors can also be contacted by phone or e-mail at:

Konstantine V. Lebedev	E-mail: klebedev@soest.hawaii.edu	Tel.: 1 (808) 956-9710
Hiroshi Yoshinari	E-mail: hyy@affrc.go.jp	Tel.: 81-45-788-7648
Nikolai A. Maximenko	E-mail: nikolai@soest.hawaii.edu	Tel.: 1 (808) 956-2584
Peter W. Hacker	E-mail: phacker@hawaii.edu	Tel.: 1 (808) 956-9312

Fax at IPRC is 1 (808) 956-9425 and at NRIFS 81-45-788-5001.

Link to the YoMaHa'07 webpage at the Asia-Pacific Data-Research Center (APDRC) is through

<http://apdrc.soest.hawaii.edu/projects/>

6. Copyright

YaMaHa'07 dataset is open for free unrestricted use, copying and distribution. The dataset is a research quality product. Errors reported to the authors by users will be published and corrected in the next update of the dataset.

Use of the data should be acknowledged in the following form:

“This study used the data of YoMaHa'07 [Lebedev et al., 2007] dataset of velocities derived from Argo float trajectories provided by APDRC/IPRC.”

Reference of this technical paper:

K. V. Lebedev, H. Yoshinari, N. A. Maximenko, and P. W. Hacker. YoMaHa'07: Velocity data assessed from trajectories of Argo floats at parking level and at the sea surface, IPRC Technical Note No. 4(2), June 12, 2007, 16p.

When copying data from YoMaHa'07, the copyright file “Copyright_070612.txt” must be also copied and kept in the same directory as the file “yomaha070612.dat”.

